Warping Torsion

In addition to shear stresses, some members carry torque by axial stresses. This is called warping torsion. This happens when the cross-section wants to warp, i.e., displace axially, but is prevented from doing so during twisting of the beam. Not all cross-sections warp, and even those that warp do not carry torque by axial stresses unless they are axially restrained at some location(s) along the member. Cross-sections that do NOT warp include axisymmetric cross-sections and thin-walled cross-sections with straight parts that intersect at one point the cross-section, such as X-shaped, T-shaped, and L-shaped cross-sections. Thin-walled closed cross-sections with constant thickness that can be circumscribed by a circle, i.e., regular polygons, such as equilateral triangles, squares, polygons, etc. also do not warp. For these cross-sections all torque is carried by shear stresses, i.e., St. Venant torsion, regardless of the boundary conditions.

Warping of I-sections

As a pedagogical introduction to warping torsion, consider a beam with an I-section, such as a wide-flange steel beam. When torsion is applied to the beam then the flanges of this cross-section experiences bending in the flange-planes. In other words, torsion induces bending about the strong axis of the flanges. When the flanges are "fixed" at some point, such as in a cantilevered beam with a fully clamped end, some of the torque is carried by axial stresses. To understand this, denote the bending moment and shear force in each flange by M and V, respectively, as shown in Figure 1.

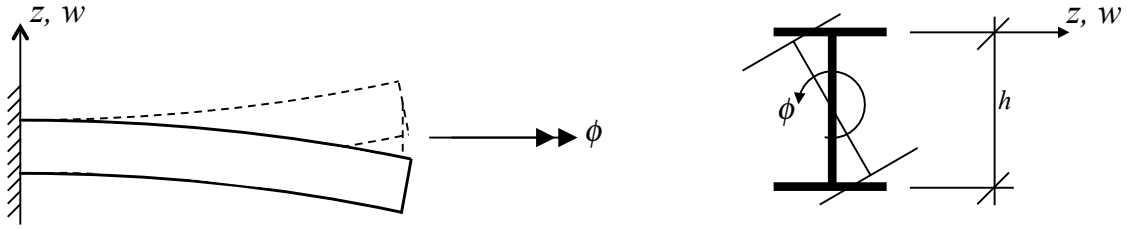

Figure 1: Warping of I-section
(z is the local axis for bending of flange, not the global z-axis of the cross-section).

The torque that the cross-section carries by bending in the flanges is:

$$T_{warping} = h \cdot V \tag{1}$$

where h is the distance between the flanges and V is positive shear force in accordance with the document on Euler-Bernoulli beam theory. That document also provides the equilibrium equation that relates shear force to bending moment, which yields:

$$V = \frac{dM}{dx} \quad \Rightarrow \quad T_{warping} = h \cdot \frac{dM}{dx} \tag{2}$$

The beam theory also provide the relationship between bending moment and flange displacement, w:

$$M = EI_{flange} \cdot \frac{d^2w}{dx^2} \quad \Rightarrow \quad T_{warping} = h \cdot EI_{flange} \cdot \frac{d^3w}{dx^3} \tag{3}$$

where I is the moment of inertia of one flange about its local strong axis. Next, Figure 1 is reviewed to determine the relationship between w and ϕ:

$$w = -\phi \cdot \frac{h}{2} \quad \Rightarrow \quad T_{warping} = -\frac{h^2}{2} \cdot EI_{flange} \cdot \frac{d^3\phi}{dx^3} \tag{4}$$

which resulted in the differential equation for warping torsion of an I-section. However, this equation is generally written in this format:

$$T_{warping} = -EC_w \cdot \frac{d^3\phi}{dx^3} \tag{5}$$

which implies that, for I-sections, the cross-sectional constant for warping is:

$$C_w = I_{flange} \cdot \frac{h^2}{2} \tag{6}$$

where it is reiterated that I_{flange} is the moment of inertia of one flange about its local strong axis.

Complete Differential Equation for Torsion

As mentioned earlier, when warping is restrained the torque is carried by both shear stresses, i.e., St. Venant torsion and axial stresses, i.e., warping torsion. Specifically, the torque from shear and axial stresses are superimposed, which leads to the following complete differential equation for torsion:

$$T = GJ \cdot \frac{d\phi}{dx} - EC_w \cdot \frac{d^3\phi}{dx^3} \tag{7}$$

When equilibrium with distributed torque along the beam, m_x, is included, i.e., $m_x = -dT/dx$, then the full differential equation reads

$$EC_w \cdot \frac{d^4\phi}{dx^4} - GJ \cdot \frac{d^2\phi}{dx^2} = m_x \tag{8}$$

Solution

The characteristic equation to obtain the homogeneous solution for the differential equation in Eq. (8) reads

$$\gamma^4 - \frac{GJ}{EC_w} \cdot \gamma^2 = 0 \tag{9}$$

The roots are 0, 0, $\sqrt{(GJ/EC_w)}$, and $-\sqrt{(GJ/EC_w)}$. Accordingly, the homogeneous solution is

$$\phi(x) = C_1 \cdot e^{\sqrt{GJ/EC_w} \cdot x} + C_2 \cdot e^{-\sqrt{GJ/EC_w} x} + C_3 \cdot x + C_4 \tag{10}$$

which guides the selection of shape functions if an "exact" stiffness matrix with both St. Venant and warping torsion is sought. Another way of expressing the solution is:

$$\phi(x) = C_1 \cdot \sinh\left(\sqrt{GJ/EC_w} \cdot x\right) + C_2 \cdot \cosh\left(\sqrt{GJ/EC_w} \cdot x\right) + C_3 \cdot x + C_4 \tag{11}$$

where the coefficients, C_i, in Eq. (10) are different from those in Eq. (11). For example, the homogeneous solution for a cantilevered beam that is fully fixed at x=0 and subjected to a torque, T_o, at x=L is:

$$\phi(x) = \frac{1}{\sqrt{GJ/EC_w}} \cdot \frac{T_o}{GJ} \cdot \begin{pmatrix} \tanh\left(\sqrt{GJ/EC_w} \cdot L\right) \cdot \left[\cosh\left(\sqrt{GJ/EC_w} \cdot x\right) - 1\right] \\ -\sinh\left(\sqrt{GJ/EC_w} \cdot x\right) + \sqrt{GJ/EC_w} \cdot x \end{pmatrix} \tag{12}$$

From this solution the torque carried by St. Venant torsion is computed by:

$$T_{St.V.}(x) = GJ \cdot \frac{d\phi}{dx} \tag{13}$$

and the torque carried by warping torsion is computed by:

$$T_{warping}(x) = -EC_w \cdot \frac{d^3\phi}{dx^3} \tag{14}$$

where $T_{St.V.}(x)+T_{warping}(x)=T_o$ for all $0<x<L$.

Bi-moment

In the theory of warping torsion the "bi-moment," B, is defined as an auxiliary quantity. This has two primary objectives. The first is to introduce a "degree of freedom" for beam elements that carry torque by restrained warping. The other objective stems from our desire to formulate a theory with a quantity that is akin to the ordinary bending moment in beam theory. In other words, the objective is to establish an equation of the form $B=EC_w\phi''$, which is analogous to the equation $M=EIw''$ from beam theory. To this end, let the bi-moment for I-sections be defined by

$$B \equiv M \cdot h \tag{15}$$

where M is again the bending moment in the flange about its strong axis. Substitution of the relationship between bending moment in the flange, w, and the flange displacement, w, from Euler-Bernoulli beam theory yields

$$B = EI \cdot \frac{d^2w}{dx^2} \cdot h \tag{16}$$

and substitution of the relationship between w and ϕ from Eq. (4) yields

$$B = -EI \cdot \frac{d^2\phi}{dx^2} \cdot \frac{h^2}{2} \tag{17}$$

which in light of Eq. (6) is written

$$B = -EC_w \cdot \frac{d^2\phi}{dx^2} \tag{18}$$

This is the desired result, which shows that Eq. (15) is the appropriate definition of the bi-moment for I-sections. It is emphasized that the bi-moment in itself is not measurable, but it serves as a convenient auxiliary quantity in the theory of warping torsion. When warping degrees of freedom are included in beam elements then the bi-moment in the force vector corresponds to the derivative of the rotation, i.e., ϕ', in the displacement vector.

Unified Bending and Torsion of Thin-walled Cross-sections

The following theory, named after Vlasov, is developed for warping torsion of thin-walled cross-sections. Because warping torsion and beam bending are both formulated in terms of axial stresses it is possible to combine the two theories. In fact, the omission of shear deformation in Euler-Bernoulli beam theory is carried over to the warping theory that is presented in the following. It is noted that no theory of warping for general "thick-walled" cross-sections is currently provided in these documents. Although this is a shortcoming, the presented theory is sufficient for many practical applications. This is because many thick-walled cross-section types are difficult to fully restrain axially. In contrast, it is easier to imagine connection designs for thin-walled cross-sections that provide sufficient axial restraint to develop torque due to axial stresses.

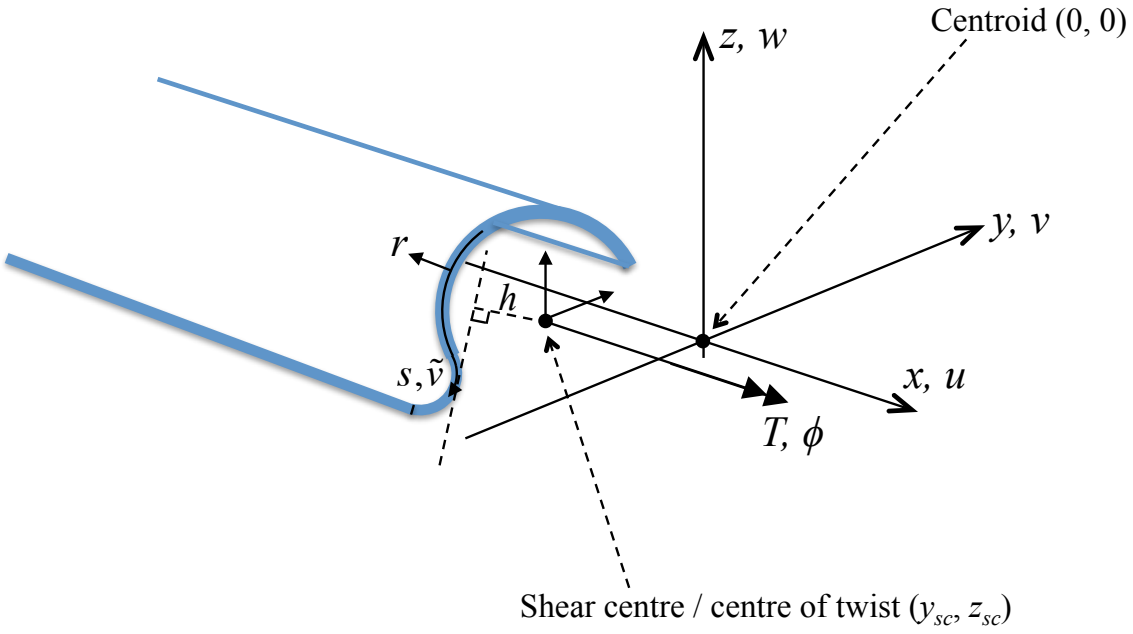

Figure 2: Beam axis system and corresponding displacements.

Kinematics

The objective in this section is to establish a relationship between axial strain, ε_x, and the displacements u, v, and w, as well as the rotation ϕ. This is achieved by first seeking a relationship between ε_x and the axial displacement, i.e., warping of the cross-section. To that end, let the coordinate s follow the centre line of the contour of the cross-section and let h denote the distance from the centre of rotation (y_{sc}, z_{sc}) to the tangent of the coordinate line s, as shown in Figure 2. The y-z-axes originate in the centroid of the cross-section and

the shear centre coordinates y_{sc} and z_{sc} are presumed to be unknown. The part of the deformation that relates to bending is governed by Euler-Bernoulli beam theory, hence the shear strain is neglected. However, for closed cross-sections the shear strain γ_{xs} from St. Venant torsion is included. Specifically, γ_{xs} is equal to the shear strain at r=0 from St. Venant theory, i.e., at the mid-plane of the cross-section profile. For open cross-sections this shear strain is zero. As a fundamental kinematics postulation it is also assumed that the cross-section retains its shape. This implies that σ_s=ε_s=0 and that the displacement in the s-direction is:

$$\tilde{v} = -v \cdot \cos(\alpha) + w \cdot \sin(\alpha) + \phi \cdot h \tag{19}$$

where v and w are the displacements of the cross-section and α is the angle between the s-axis and the y-axis. The contributions to Eq. (19) are illustrated in Figure 3. This figure also shows how $\sin(\alpha)$ and $\cos(\alpha)$ are expressed in terms of the differentials ds, dy, and dz are established, namely:

$$\begin{aligned} \frac{dy}{ds} &= -\cos(\alpha) \\ \frac{dz}{ds} &= \sin(\alpha) \end{aligned} \tag{20}$$

Substitution of Eq. (20) into Eq. (19) yields:

$$\tilde{v} = v \cdot \frac{dy}{ds} + w \cdot \frac{dz}{ds} + \phi \cdot h \tag{21}$$

which expresses that the cross-section retains its shape during deformation.

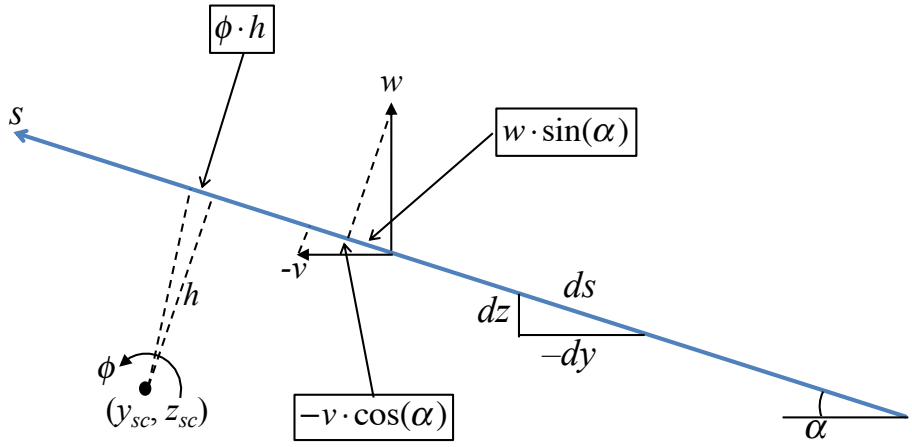

Figure 3: Contributions to the displacement along the s-axis.

Because the boundary value problem at hand relates to axial strains, the following equation is the fundamental kinematics equation:

$$\varepsilon_x = \frac{du}{dx} \tag{22}$$

Next, an expression for u is sought, namely the infinitesimal axial displacement, i.e., warping, between two infinitesimally close points in the cross-section. To this end, it is

noted that the shear flow in closed cross-sections due to shear force was determined by using the following expressions:

$$\gamma = \frac{du}{ds} \qquad \Rightarrow \qquad du = \gamma \cdot ds \tag{23}$$

It is also recalled that the derivation of *du* in St. Venant torsion for closed cross-sections was determined by including rotation of the cross-section:

$$\gamma_{xs} = \frac{d\tilde{v}}{dx} + \frac{du}{ds} \qquad \Rightarrow \qquad du = \gamma_{xs} \cdot ds - \frac{d\tilde{v}}{dx} \cdot ds = \gamma_{xs} \cdot ds - \frac{d\phi}{dx} \cdot h \cdot ds \tag{24}$$

where the last term represents the axial displacement, i.e., warping, due to the rotation, ϕ. The kinematics of Eq. (24) is also utilized in the following, but the expression for $\tilde{v}$ includes all the terms in Eq. (21). Substitution of Eq. (21) into Eq. (24) yields:

$$du = -\frac{\mathrm{d}v}{\mathrm{d}x} \cdot dy - \frac{\mathrm{d}w}{\mathrm{d}x} \cdot dz - \left(\frac{\mathrm{d}\phi}{\mathrm{d}x} \cdot h - \gamma_{xs} \right) \cdot ds \tag{25}$$

However, γ_{xs} is non-zero only for closed cross-sections, and closed cross-sections are addressed later. Hence, for open cross-sections:

$$du = -\frac{\mathrm{d}v}{\mathrm{d}x} \cdot dy - \frac{\mathrm{d}w}{\mathrm{d}x} \cdot dz - \frac{\mathrm{d}\phi}{\mathrm{d}x} \cdot h \cdot ds \tag{26}$$

The *u*-displacement at any point in the cross-section is obtained by summing the infinitesimal contributions in Eq. (26). In other words, integration along the *y*, *z*, and *s* directions yields the complete expression for axial displacement at a point in the cross-section:

$$u(y,z) = u_o - \frac{\mathrm{d}v}{\mathrm{d}x} \cdot y - \frac{\mathrm{d}w}{\mathrm{d}x} \cdot z - \frac{\mathrm{d}\phi}{\mathrm{d}x} \cdot \int h\, ds \tag{27}$$

where u_o is the integration constant, i.e., the axial displacement at the neutral axis. More important in this document is the last term; it represents the axial displacement, i.e., warping, caused by torsion. The function that quantifies this warping is denoted Ω. Based on the derivations above the "omega function" is defined as

$$\Omega(s) \equiv \int h\, ds \tag{28}$$

so that Eq. (27) can be written

$$u(y,z) = u_o - v' \cdot y - w' \cdot z - \phi' \cdot \Omega \tag{29}$$

Eq. (29) shows that Ω is the warping of the cross-section due to a unit twist rate. This means that, physically, the Ω diagram is the varying axial displacement within the cross-section caused by ϕ'=1. The procedure to determine the omega diagram is given later in this document. Combining Eq. (22) and Eq. (27) yields the final kinematics equation:

$$\varepsilon_x = \frac{\mathrm{d}u}{\mathrm{d}x} - \frac{\mathrm{d}^2v}{\mathrm{d}x^2} \cdot y - \frac{\mathrm{d}^2w}{\mathrm{d}x^2} \cdot z - \frac{\mathrm{d}^2\phi}{\mathrm{d}x^2} \cdot \Omega \tag{30}$$

where u_o has been renamed to u to match the typical notation for truss members.

Revised Kinematics for Cross-sections with One Cell

Above it was postulated that $\gamma_{xs}=0$, which is only true at the mid-thickness of open-cross-sections. In the "walls" of a cell in a closed cross-section the kinematics expressed in Eq. (26) has the following expanded form:

$$du = -v' \cdot dy - w' \cdot dz - \left(\phi' \cdot h - \gamma_{xs}\right) ds \tag{31}$$

It is desirable to express γ_{xs} in terms of ϕ' so that the latter can be pulled outside the parenthesis in Eq. (31). This is achieved by utilizing equations from the theory of St. Venant torsion. The material law is

$$\gamma_{xs} = \frac{\tau_{xs}}{G} \tag{32}$$

From St. Venant torsion the stress in the wall of a cell is

$$\tau_{xs} = \frac{K}{t} \tag{33}$$

where K is the amplitude of the stress function and t is the thickness of the wall. For single-cell cross-sections without free flanges that amplitude is determined from the equation

$$T = 2 \cdot V = 2 \cdot K \cdot A_m \tag{34}$$

where V is the volume under the stress function. Consequently, the shear strain for one-celled cross-sections without free flanges is

$$\gamma_{xs} = \frac{\tau_{xs}}{G} = \frac{K}{G \cdot t} = \frac{T}{G \cdot t \cdot 2 \cdot A_m} = \frac{J}{2 \cdot t \cdot A_m} \cdot \phi' \tag{35}$$

where $T=GJ\phi'$ is employed in the last equality. That means the omega function for one-celled cross-sections without free flanges is

$$\Omega(s) = \int \left(h - \frac{J}{2 \cdot t \cdot A_m} \right) ds \tag{36}$$

The new term is referred to as the "shear radius:"

$$\overline{h} = \frac{J}{2 \cdot t \cdot A_m} \tag{37}$$

Revised Kinematics for Cross-sections with Many Cells and/or Free Flanges

For more complex cross-sections it is necessary to revisit the calculation of the shear strain at the mid-thickness of the cell walls. Eqs. (32) and (33) remain valid:

$$\gamma_{xs} = \frac{K}{G \cdot t} \tag{38}$$

However, the calculation of K differs from Eq. (34). One reason is the contribution from free flanges, i.e., parts of the cross-section whose shear stress mimics that of open cross-

sections, must be included. Also, the value of K, i.e., the amplitude of the stress function in cells, is in general different for different cell walls. This fact is illustrated in Figure 4, together with a view of the stress functions in the open parts of the cross-section, i.e., the free flanges.

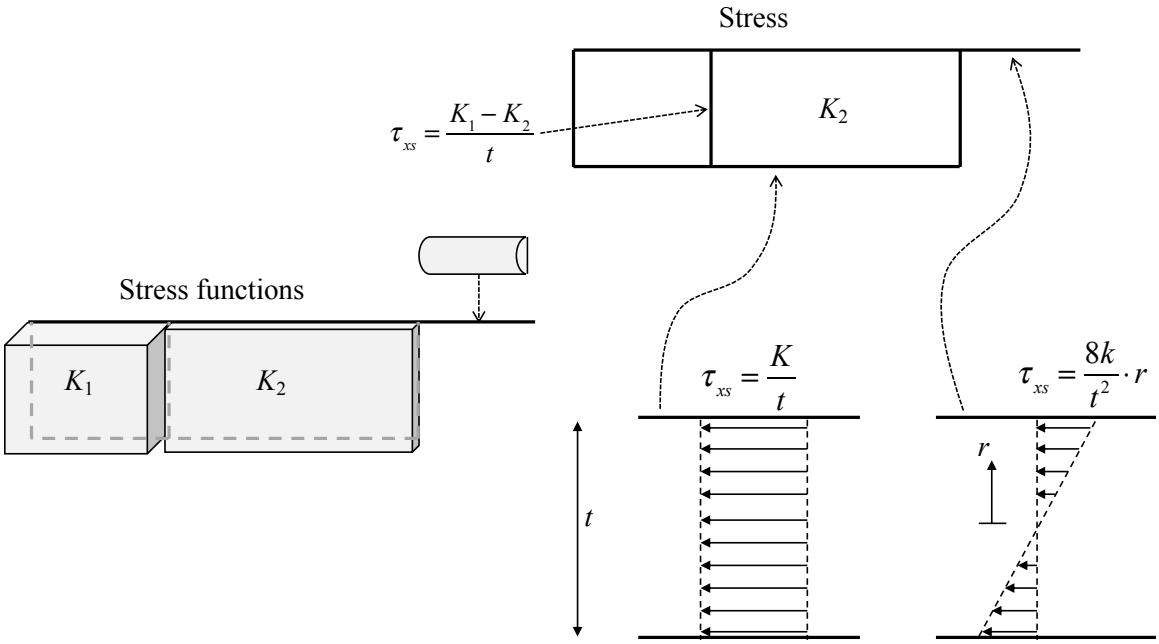

Figure 4: Stress and stress functions for multi-cell cross-section with free flanges.

Now the total torque is carried by several stress functions:

$$T = 2 \cdot \int_A P(r,s)\,dA = \sum_{i=1}^{N_{cells}} 2 \cdot K_i \cdot (A_m)_i + 2 \cdot \frac{2}{3} \cdot k \cdot \sum_{j=1}^{N_{flanges}} t_j \cdot b_j \tag{39}$$

where A_m=cell area, b=length of free flanges, and t=thickness of free flanges. For example, the value of K in the left-most wall of the two-cell cross-section with one free flange shown in Figure 4 is

$$K_1 = \frac{T}{2 \cdot A_{m1}} - \frac{K_2 \cdot A_{m2}}{A_{m1}} - \frac{2 \cdot k \cdot t_{flange} \cdot b}{3 \cdot A_{m1}} \tag{40}$$

The presence of the torque, T, is necessary in every term, not only the first term, so that $T=GJ\phi'$ can be used to express γ_{xs} in terms of ϕ' in order to obtain a workable expression for the omega diagram. In other words, it is necessary to express K_2 and k in terms of T. this can be done by recording the percentage of the total torque, T, carried by each part of the cross-section. That is possible, using Eq. (39), because the values of K_i and k are known from the St. Venant torsion analysis. Suppose the torque carried by Cell 2 is C_2T. That implies $2K_2A_{m2}=C_2T$ and, thus

$$K_2 = \frac{C_2 \cdot T}{2 \cdot A_{m2}} \tag{41}$$

Similarly, for the free flange:

$$k = \frac{3 \cdot C_{flange} \cdot T}{4 \cdot t_{flange} \cdot b} \tag{42}$$

Substitution into Eq. (38) yields the sought shear strain:

$$\gamma_{xs} = \left(\frac{J}{2 \cdot t_{wall} \cdot A_{m1}} \cdot \left(1 - C_2 - C_{flange}\right) \right) \cdot \phi' \tag{43}$$

That means the omega function for the cross-section in Figure 4 is

$$\Omega(s) = \int \left(h - \frac{J}{2 \cdot t_{wall} \cdot A_{m1}} \cdot \left(1 - C_2 - C_{flange}\right) \right) ds \tag{44}$$

In other words, for complex closed cross-sections the omega diagram around a cell is established using x% of the shear radius defined in Eq. (37), where x is the percentage of the total torque carried by that cell. Because of the fundamental equation $T=GJ\phi'$ the contributions to T from each cross-section part matches the contributions to J. Thus, the sought percentage can be determined during the calculation of J in St. Venant torsion.

Material Law

Hooke's law provides the relationship between axial stress and axial strain:

$$\sigma_x = E \cdot \varepsilon_x \tag{45}$$

Section Integration

Integration of axial stress, which is positive in tension, over the cross-section yields the axial force, which is also positive in tension:

$$N = \int_A \sigma_x \, dA \tag{46}$$

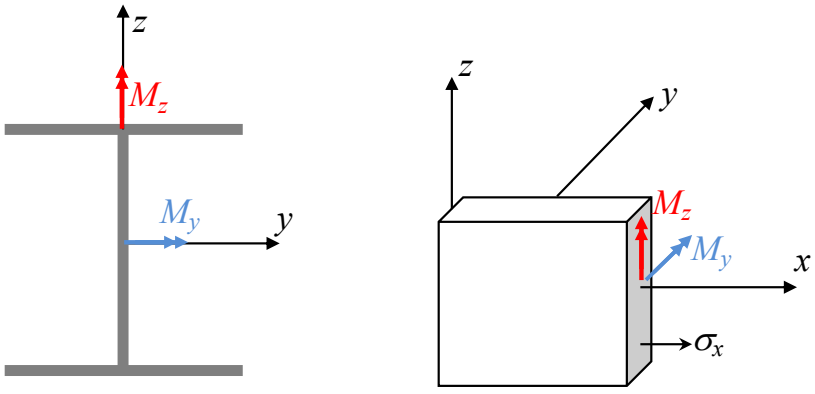

Figure 5: Determining the signs of bending moments.

In the elementary 2D Euler-Bernoulli beam theory it is often postulated that a "positive bending moment" gives tension at the bottom. That statement is awkward in the 3D beam presented here, and Figure 5 presents a better foundation for determining the signs of the bending moment stress resultants. Integration of axial stress, which is positive in tension, multiplied by the distance, y, from the centroid yields the bending moment

$$M_z = -\int_A \sigma_x \cdot y \, dA \tag{47}$$

Similarly, positive tensile stress where z is positive contributes to positive moment about the y-axis:

$$M_y = \int_A \sigma_x \cdot z \, dA \tag{48}$$

Integration of axial stress multiplied by the previously defined quantity Ω is defined as the "bi-moment:"

$$B \equiv -\int_A \sigma_x \cdot \Omega \, dA \tag{49}$$

Equilibrium

Distributed axial load along the beam is related to the axial force by the following equilibrium equation:

$$q_x = -\frac{dN}{dx} \tag{50}$$

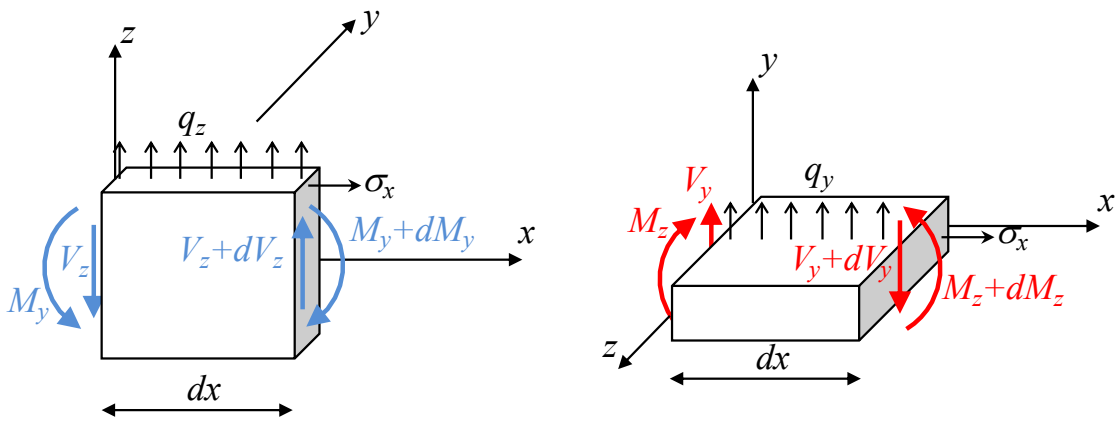

Figure 6: Equilibrium for infinitesimally small beam element, extending Figure 5.

Figure 6 shows an infinitesimally long portion of a beam element whose equilibrium equations are now sought. The direction of the bending moments is determined by Figure 5, implying that M_y is the bending moment about the y-axis and M_z is the bending moment about the z-axis. First addressing the left-hand side of Figure 6, equilibrium in the z-direction yields

$$q_z = -\frac{dV_z}{dx} \tag{51}$$

Moment equilibrium about the gray-shaded side on the left-hand side of Figure 6 yields

$$V_z = \frac{dM_y}{dx} \tag{52}$$

For the shear force shown in the right-hand side of Figure 6, it is necessary to specify whether V_y means the shear force in the y-direction, or the shear force the in the direction dictated by equilibrium. The latter choice is made here, as shown in the right-hand side of Figure 6. Equilibrium in the y-direction yields

$$q_y = \frac{dV_y}{dx} \tag{53}$$

Moment equilibrium about the gray-shaded side on the right-hand side of Figure 6 yields

$$V_y = \frac{dM_z}{dx} \tag{54}$$

Finally, equilibrium for distributed torque along the beam yields:

$$m_x = -\frac{dT}{dx} \tag{55}$$

Differential Equations

Substitution of the kinematics equation in Eq. (30) into the material law in Eq. (45) yields:

$$\sigma_x = E \cdot \frac{\mathrm{d}u}{\mathrm{d}x} - E \cdot \frac{\mathrm{d}^2 v}{\mathrm{d}x^2} \cdot y - E \cdot \frac{\mathrm{d}^2 w}{\mathrm{d}x^2} \cdot z - E \cdot \frac{\mathrm{d}^2 \phi}{\mathrm{d}x^2} \cdot \Omega \tag{56}$$

Substitution of Eq. (56) into the section integration Eqs. (46) to (49) yields the following set of equations (Weberg 1970):

$$\begin{Bmatrix} N \\ M_z \\ -M_y \\ -B \end{Bmatrix} = E \cdot \begin{bmatrix} \int_A dA & -\int_A y\,dA & -\int_A z\,dA & -\int_A \Omega\,dA \\ -\int_A y\,dA & \int_A y^2\,dA & \int_A y \cdot z\,dA & \int_A y \cdot \Omega\,dA \\ -\int_A z\,dA & \int_A y \cdot z\,dA & \int_A z^2\,dA & \int_A z \cdot \Omega\,dA \\ -\int_A \Omega\,dA & \int_A y \cdot \Omega\,dA & \int_A z \cdot \Omega\,dA & \int_A \Omega^2\,dA \end{bmatrix} \begin{Bmatrix} \frac{du}{dx} \\ \frac{d^2 v}{dx^2} \\ \frac{d^2 w}{dx^2} \\ \frac{d^2 \phi}{dx^2} \end{Bmatrix} \tag{57}$$

where symmetry is observed. Under certain conditions described shortly, the equations become decoupled and reduces to:

$$N = EA \cdot \frac{du}{dx} \tag{58}$$

$$M_z = EI_z \frac{d^2 v}{dx^2} \tag{59}$$

$$M_y = -EI_y \frac{d^2 w}{dx^2} \tag{60}$$

$$B = -EC_w \frac{d^2\phi}{dx^2} \tag{61}$$

where the diagonal components of the matrix in Eq. (57) have been named as follows:

$$A = \int_A \mathrm{d}A \tag{62}$$

$$I_z = \int_A y^2 \, dA \tag{63}$$

$$I_y = \int_A z^2 \, dA \tag{64}$$

$$C_\omega = \int_A \Omega^2 \, dA \tag{65}$$

The complete differential equation for axial deformation is obtained by combining Eqs. (50) and (58):

$$q_x = -EA \cdot \frac{d^2u}{dx^2} \tag{66}$$

The complete differential equation for bending about the *z*-axis is obtained by combining Eqs. (53), (54), and (59):

$$q_y = EI_z \frac{d^4v}{dx^4} \tag{67}$$

The complete differential equation for bending about the *y*-axis is obtained by combining Eqs. (51), (52), and (60):

$$q_z = EI_y \frac{d^4w}{dx^4} \tag{68}$$

Conditions for Decoupling

For the system of equations in Eq. (57) to be decoupled, the six off-diagonal elements of the coefficient matrix must be zero. These six conditions form an important part of the cross-section analysis. In fact, they determine the following six unknowns of the cross-section:

1. y_o = y-coordinate of the centroid
2. z_o = z-coordinate of the centroid
3. θ_o = orientation of the principal axes
4. C = normalizing constant for the Ω-diagram
5. y_{sc} = y-coordinate of the shear centre
6. z_{sc} = z-coordinate of the shear centre

Specifically, the coordinates of the centroid of the cross-section are determined by:

$$\int_A y \ \mathrm{d}A = \int_A z \ \mathrm{d}A = 0 \tag{69}$$

The orientation of the principal axes are determined by:

$$\int_A y \cdot z \ \mathrm{d}A = 0 \tag{70}$$

The normalizing constant for the Ω-diagram is determined by:

$$\int_A \Omega \ \mathrm{d}A = 0 \tag{71}$$

The shear centre coordinates are determined by:

$$\int_A y \cdot \Omega \ \mathrm{d}A = \int_A z \cdot \Omega \ \mathrm{d}A = 0 \tag{72}$$

Differential Equation with St. Venant Torsion

The derivation of the differential equation that combines St. Venant torsion and warping torsion starts with the definition of the stress resultant:

$$T = \int_A \tau_{xs} \cdot t \cdot h \, dA = \int_A q_s \cdot h \, ds = \int_A q_s \, d\Omega = \left[q_s \cdot \Omega \right]_\Gamma - \int_A \Omega \, dq_s \tag{73}$$

where q_s is the shear flow and the boundary term $[q_s \Omega]_\Gamma$ from integration by parts is zero. Because shear strains are omitted from the warping theory it is necessary to employ equilibrium to recover the shear flow. With reference to Figure 7, equilibrium yields:

$$d\sigma_x \cdot ds \cdot t + d\tau_{xs} \cdot dx \cdot t = 0 \quad \Rightarrow \quad \frac{d\sigma_x}{dx} \cdot t + \frac{d\tau_{xs}}{ds} \cdot t = 0 \quad \Rightarrow \quad \frac{dq_s}{ds} = -\frac{d\sigma_x}{dx} \cdot t \tag{74}$$

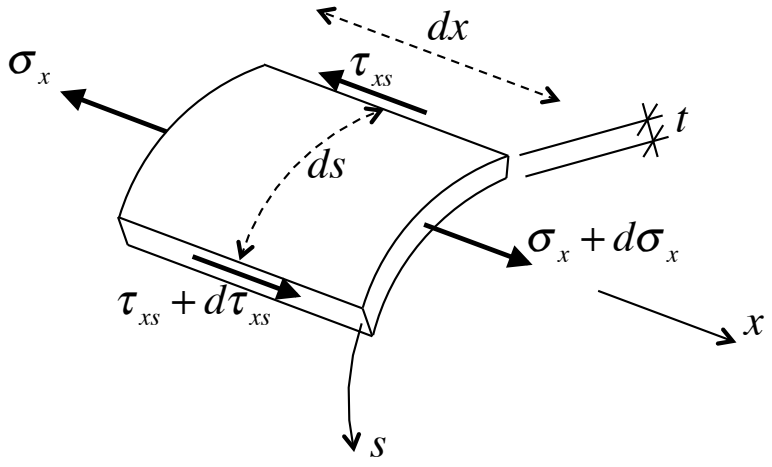

Figure 7: Equilibrium to recover shear stresses.

Substitution of Eq. (74) into Eq. (73) yields:

$$T = -\int_A \Omega \, dq_s = \int_A \Omega \cdot \frac{d\sigma_x}{dx} \cdot t \, ds = \int_A \Omega \cdot \frac{d\sigma_x}{dx} \, dA = \frac{d}{dx} \int_A \Omega \cdot \sigma_x \, dA = -\frac{dB}{dx} \tag{75}$$

Adding the torque carried by shear stresses, i.e., $T=GJ(d\phi/dx)$ and employing Eq. (61) yields:

$$T = GJ \cdot \frac{d\phi}{dx} - EC_w \frac{d^3\phi}{dx^3} \tag{76}$$

Adding equilibrium with distributed torque from Eq. (55) yields the complete differential equation for St. Venant torsion and warping torsion:

$$m_x = EC_w \frac{d^4\phi}{dx^4} - GJ \cdot \frac{d^2\phi}{dx^2} \tag{77}$$

The solution to this differential equation was presented in Eq. (10).

Determination of the Omega Diagram

The quantity Ω varies over the cross-section, and is proportional to the axial warping of the cross-section. For open cross-sections, Ω is defined as

$$\Omega \equiv \int h\, ds \tag{78}$$

where h is the distance from the centre of rotation to the tangent of the cross-section coordinate s. For closed cross-sections, Ω is defined as

$$\Omega \equiv \int \left(h - \overline{h}\right) ds \tag{79}$$

where the "shear radius" is, for cross-sections with once cell:

$$\overline{h} = \frac{J}{2 \cdot t \cdot A_m} \tag{80}$$

The practical determination of the Ω-diagram is based on the conditions

$$\int_A \Omega \ \mathrm{d}A = 0 \tag{81}$$

and

$$\int_A y \cdot \Omega \ \mathrm{d}A = \int_A z \cdot \Omega \ \mathrm{d}A = 0 \tag{82}$$

In words, the final Ω-diagram must be "normalized" and it must be drawn about the shear centre, (y_{sc}, z_{sc}), of the cross-section. In order to arrive at the final diagram, a trial diagram is first drawn. Thereafter, the trial diagram is modified to obtain the final one. For this purpose, it is useful to establish an expression that relates the Ω-diagram drawn about an arbitrary trial point, here labelled (y_{trial}, z_{trial}), to another diagram drawn about the shear centre. Since the Ω-values consist of accumulated double sector areas it is of interest to study a generic infinitesimal contribution. To this end, Figure 8 identifies by gray-shading the Ω-diagram contributions for an infinitesimal length ds of the cross-section. The double area of the sector that originates in (y_{sc}, z_{sc}) is

$$d\Omega_{sc} = dy \cdot \left(z - z_{sc}\right) - dz \cdot \left(y - y_{sc}\right) \tag{83}$$

The double area of the sector that originates in (y_Q, z_Q) is

$$d\Omega_{trial} = dy \cdot (z - z_{trial}) - dz \cdot (y - y_{trial}) \tag{84}$$

The difference between the two Ω-diagram contributions in Figure 8 is

$$d\Omega_{sc} - d\Omega_{trial} = (y_{sc} - y_{trial}) \cdot dz - (z_{sc} - z_{trial}) \cdot dy \tag{85}$$

Integration of infinitesimal contributions yield the expression for the difference in Ω-diagrams:

$$\Omega_{sc} - \Omega_{trial} = (y_{sc} - y_{trial}) \cdot z - (z_{sc} - z_{trial}) \cdot y + C \tag{86}$$

where C is the integration constant. Rearranging and renaming Ω_{sc} to Ω yields:

$$\Omega = \Omega_{trial} + (y_{sc} - y_{trial}) \cdot z - (z_{sc} - z_{trial}) \cdot y + C \tag{87}$$

which is the expression for the final Ω-diagram once C, y_{sc}, and z_{sc} are known.

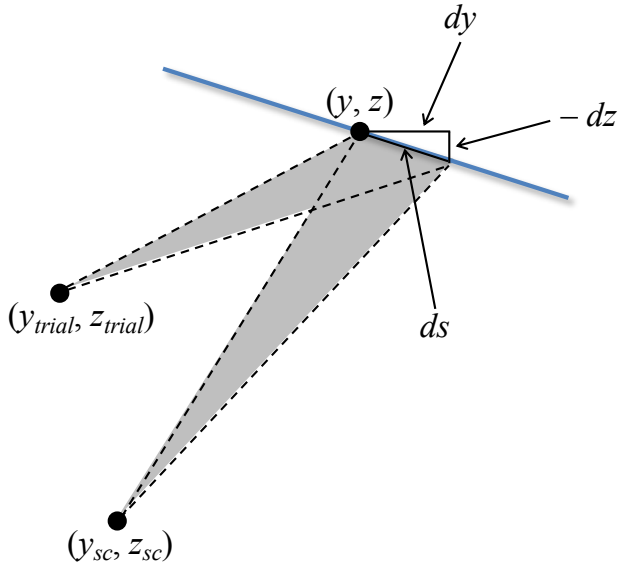

Figure 8: Relationship between two Ω-diagrams.

The integration constant, C, normalizes the Ω-diagram and is determined by requiring the integral of the Ω-diagram in Eq. (87) to be zero according to Eq. (71):

$$\int_A \Omega \, dA = \int_A \Omega_{trial} \, dA + \int_A C \, dA = 0 \quad \Rightarrow \quad C = -\frac{\int_A \Omega_{trial} \, dA}{A} \tag{88}$$

where terms cancel in the integration because y and z originate at the centroid of the cross-section. The shear centre coordinates y_{sc} and z_{sc} are determined by requiring the integrals in Eq. (72) of the Ω-diagram in Eq. (87) to vanish:

$$\int_A y\cdot\Omega\,dA=\int_A y\cdot\Omega_{trial}\,dA-\left(z_{sc}-z_{trial}\right)\cdot\int_A y^2\,dA=0\quad\Rightarrow\quad z_{sc}-z_{trial}=\frac{\int_A y\cdot\Omega_{trial}\,dA}{I_z}\tag{89}$$

$$\int_A z\cdot\Omega\,dA=\int_A z\cdot\Omega_{trial}\,dA+\left(y_{sc}-y_{trial}\right)\cdot\int_A z^2\,dA=0\quad\Rightarrow\quad y_{sc}-y_{trial}=-\frac{\int_A z\cdot\Omega_{trial}\,dA}{I_y}\tag{90}$$

where terms cancel in the integration because y and z are principal axes of the cross-section. In summary, the following procedure is suggested for the determination of C, y_{sc}, z_{sc}, and ultimately the Ω-diagram:

1. Select an arbitrary point, (y_{trial}, z_{trial}), in the cross-section
2. Draw the trial Ω_{trial}-diagram about (y_{trial}, z_{trial}), i.e., gather contributions to the integral along cross-section parts by a clockwise "radar sweep" about the trial point, while ensuring that the Ω_{trial}-diagram is continuous; notice, contributions that are gathered in a clockwise "sweep" are positive, while those gathered in a counter-clockwise sweep are negative
3. Determine C by Eq. (88)
4. Determine z_{sc} by Eq. (89)
5. Determine y_{sc} by Eq. (90)
6. Determine final Ω-diagram by Eq. (87)

When addressing Item 2 above for closed cross-sections, then it may at first appear that a discontinuous Ω-diagram will be obtained. In other words, whichever start-point is selected in the cross-section, it appears unlikely that the Ω-value will return to zero after circumnavigating the cell. However, the following derivation shows that this will always occur. According to Eq. (79), the end-value of the Ω-coordinate after circumnavigating a cell is:

$$\begin{aligned}\Omega&=\oint h\,ds-\oint\frac{J}{2\cdot t\cdot A_m}ds=2\cdot A_m-\frac{J}{2\cdot A_m}\cdot\oint\frac{1}{t}ds\\&=2\cdot A_m-\frac{\left(\dfrac{4\cdot A_m^2}{\oint\frac{1}{t}ds}\right)}{2\cdot A_m}\cdot\oint\frac{1}{t}ds=2\cdot A_m-2\cdot A_m=0\end{aligned}\tag{91}$$

Cross-section Constant for Warping Torsion

For general thin-walled cross-sections the warping torsion constant is

$$C_w=\int_A\Omega^2\,dA\tag{92}$$

where Ω is the omega-diagram for the cross-section. When evaluating this expression it can be helpful to employ the quick-integration formulas that are developed for the virtual work integral

$$\Delta = \int_0^L \delta M \cdot \frac{M}{EI} dx \tag{93}$$

When using this approach, the quick-integration formulas are applied to the different parts of the cross-section individually, followed by summation, just like virtual work is added for different parts of the structure.

Axial Stresses

The key characteristic of warping torsion is the carrying of torque by axial stresses. Analogous to the Euler-Bernoulli beam theory, axial stresses are obtained by first combining the kinematics of Eq. (30) with the material law in Eq. (45), and thereafter substituting Eqs. (58)-(61), which yields

$$\begin{aligned} \sigma_x &= E \cdot \frac{\mathrm{d}u}{\mathrm{d}x} - E \cdot \frac{\mathrm{d}^2 v}{\mathrm{d}x^2} \cdot y - E \cdot \frac{\mathrm{d}^2 w}{\mathrm{d}x^2} \cdot z - E \cdot \frac{\mathrm{d}^2 \phi}{\mathrm{d}x^2} \cdot \Omega \\ &= E \cdot \left(\frac{N}{EA} \right) - E \cdot \left(\frac{M_z}{EI_z} \right) \cdot y - E \cdot \left(-\frac{M_y}{EI_y} \right) \cdot z - E \cdot \left(-\frac{B}{EC_w} \right) \cdot \Omega \\ &= \frac{N}{A} - \frac{M_z}{I_z} \cdot y + \frac{M_y}{I_y} \cdot z + \frac{B}{C_w} \cdot \Omega \end{aligned} \tag{94}$$

It is observed that the omega diagram shows the distribution of axial stresses in the cross-section due to torsion when warping is restrained.

Shear Stresses

Although the principal characteristic of warping torsion is torque being carried by axial stresses, shear stresses also appear in warping torsion. As in ordinary beam theory, shear stresses are not part of the boundary value problem but they are recovered by equilibrium. With reference to Figure 7, equilibrium yields:

$$d\sigma_x \cdot ds \cdot t + d\tau_{xs} \cdot dx \cdot t = 0 \tag{95}$$

Dividing through by dx and ds yields

$$\frac{d\sigma_x}{dx} \cdot t + \frac{d\tau_{xs}}{ds} \cdot t = 0 \tag{96}$$

Furthermore, recognizing that the shear flow is $q_s = t_{xs} \cdot t$ yields

$$\frac{dq_s}{ds} = -\frac{d\sigma_x}{dx} \cdot t \tag{97}$$

The shear flow is then obtained by integration:

$$\begin{aligned} q_s &= \int_0^s \frac{dq_s}{ds}\cdot ds = -\int_0^s t\cdot\frac{d\sigma_x}{dx}ds = -\int_0^s \frac{d\sigma_x}{dx}dA \\ &= -\int_0^s \left(\frac{dN}{dx}\cdot\frac{1}{A} - \frac{dM_z}{dx}\cdot\frac{1}{I_z}\cdot y + \frac{dM_y}{dx}\cdot\frac{1}{I_y}\cdot z + \frac{dB}{dx}\cdot\frac{1}{C_w}\cdot\Omega \right) dA \\ &= -\frac{dN}{dx}\cdot\frac{1}{A}\cdot A_s + \frac{V_y}{I_z}\cdot Q_y - \frac{V_z}{I_y}\cdot Q_z - \frac{dB}{dx}\cdot\frac{1}{C_w}\cdot Q_\Omega \end{aligned} \tag{98}$$

where the following definitions are made:

$$A_s = \int_0^s dA = \int_0^s t\,ds \tag{99}$$

$$Q_y = \int_0^s y\,dA = \int_0^s y\cdot t\,ds \tag{100}$$

$$Q_z = \int_0^s z\,dA = \int_0^s z\cdot t\,ds \tag{101}$$

$$Q_\Omega = \int_0^s \Omega\,dA = \int_0^s \Omega\cdot t\,ds \tag{102}$$

Eq. (98) shows that the shear flow due to torsion-induced warping is

$$q_s = -\frac{B'}{C_w}Q_\Omega \tag{103}$$

From Eq. (18), the derivative of the bi-moment is

$$B' = -EC_w\cdot\phi''' \tag{104}$$

which coincides with the expression for the warping torque, $T_{warping}$, in Eq. (5). For the case of a cantilevered beam, completely restrained against warping at the free end, the maximum warping torque appears at the fixed end. Furthermore, the warping torque equals the applied torque; hence, $B'=T_{warping}=T$. In that case, the shear stress due to warping torsion is

$$q_s = -\frac{T}{C_w}Q_\Omega \tag{105}$$

The determination of shear stresses from warping torsion in closed cross-sections is a "statically indeterminate" problem, similar to what is encountered for closed cross-sections subjected to shear force. It is also emphasized that a cross-section that carries torque both by the St. Venant effect and the warping effect will carry that torque by the shear stresses shown in Figure 9. The figure shows the contribution from St. Venant torsion as it is for an open cross-section. For closed cross-sections, both shear stresses are distributed uniformly over the thickness.

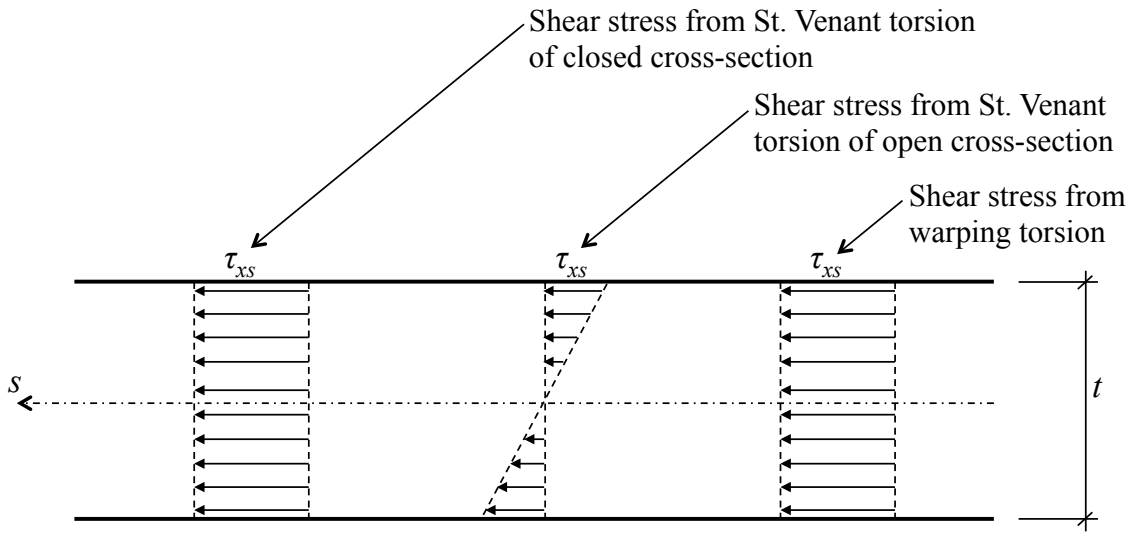

Figure 9: Shear stress from St. Venant and warping torsion.

Modified Theory for Closed Cross-sections

The theory presented above is now modified with a new expression u, i.e., with a new formulation of the warping (Hals 1993). The focus remains on thin-walled cross-sections, and the correction is particularly aimed at improving the results for closed cross-sections. A key characteristic of the modified theory is that both shear and axial stresses are considered in the same boundary value problem. This is new, because only axial strains and stresses are considered in Euler-Bernoulli beam theory and the warping theory above. Conversely, the St. Venant warping theory is formulated in terms of shear stresses. Figure 10 is included to emphasize the combined boundary value problem that is now considered.

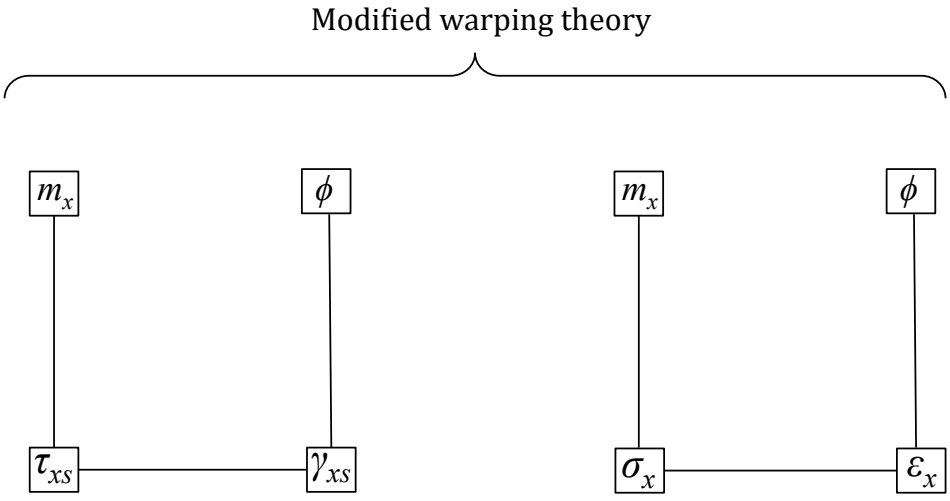

Figure 10: Combined BVP for warping torsion considering both shear and axial strains.

The key modification in this theory is a revision of Eq. (27), while Eq. (19) is maintained. The warping due to rotation of the cross-section is now written

$$u(y,z) = -F(x) \cdot \Omega \tag{106}$$

instead of

$$u(y,z) = -\frac{\mathrm{d}\phi}{\mathrm{d}x} \cdot \Omega \tag{107}$$

The function $F(x)$ is so far unknown and generally different from ϕ'.

Boundary Value Problem for Shear

Kinematic considerations yield the shear strain:

$$\gamma_{xs} = \frac{d\tilde{v}}{dx} + \frac{du}{ds} = \frac{d\phi}{dx} \cdot h - F \cdot \frac{d\Omega}{ds} \tag{108}$$

Material law added to the kinematics equation yields:

$$\tau_{xs} = G \cdot \left(\frac{d\phi}{dx} \cdot h - F \cdot \frac{d\Omega}{ds} \right) \tag{109}$$

Section integration of shear stresses around the cell yields the total torque:

$$\begin{aligned} T &= \oint \tau_{xs} \cdot t \cdot h \cdot ds = \oint G \cdot \left(\frac{d\phi}{dx} \cdot h - F \cdot \frac{d\Omega}{ds} \right) \cdot t \cdot h \cdot ds \\ &= G \cdot \frac{d\phi}{dx} \cdot \oint t \cdot h^2 \cdot ds - G \cdot F \cdot \oint \frac{d\Omega}{ds} \cdot t \cdot h \cdot ds \end{aligned} \tag{110}$$

This equation can be simplified. First, the following definition is made:

$$J_h = \oint t \cdot h^2 \cdot ds = \int_A h^2 \cdot dA \tag{111}$$

Second, in accordance with the definition of the omega diagram it is recognized that

$$\frac{d\Omega}{ds} = \left(h - \overline{h} \right) \tag{112}$$

This means that Eq. (110) takes the form

$$T = G \cdot \frac{d\phi}{dx} \cdot J_h - G \cdot F \cdot \oint h^2 \cdot t \cdot ds + G \cdot F \cdot \oint \overline{h} \cdot h \cdot t \cdot ds \tag{113}$$

Interestingly, the last term can be rewritten in terms of the cross-sectional constant for St. Venant warping. Introducing Eq. (37) yields:

$$\oint h \cdot \overline{h} \cdot t \cdot ds = \oint h \cdot \left(\frac{J}{2 \cdot t \cdot A_m} \right) \cdot t \cdot ds = \frac{J}{2 \cdot A_m} \cdot \underbrace{\oint h \cdot ds}_{2 \cdot A_m} = J \tag{114}$$

Thus, Eq. (113) turns into:

$$T = G \cdot J_h \cdot \frac{d\phi}{dx} - G \cdot F \cdot (J_h - J) \tag{115}$$

If the cross-section has protruding flanges then those are added according to the basic St. Venant formula T=GJϕ':

$$T = G \cdot \frac{d\phi}{dx} \cdot (J_h + J_{flanges}) - G \cdot F \cdot (J_h - J) \tag{116}$$

Finally, after having employed kinematics, material law, and section integration, equilibrium with applied distributed torque is added in accordance with Eq. (55), which substituted into Eq. (116) yields the differential equation:

$$G \cdot (J_h + J_{flanges}) \cdot \frac{d^2\phi}{dx^2} - G \cdot (J_h - J) \cdot \frac{dF}{dx} = -m_x \tag{117}$$

Boundary Value Problem for Axial

Kinematic considerations without bending and truss action yield the axial strain:

$$\varepsilon_x = -\frac{dF}{dx} \cdot \Omega \tag{118}$$

Material law added to the kinematic equation yields:

$$\sigma_x = -E \cdot \frac{dF}{dx} \cdot \Omega \tag{119}$$

Point-wise equilibrium in solid mechanics is expressed in index notation as $\sigma_{ij,i}+p_j=0$. This leads to the following equilibrium equation for points on the cross-section contour:

$$t \cdot \sigma_{x,x} + t \cdot \tau_{xs,s} + p_x = 0 \tag{120}$$

where p_x is the force-intensity in the x-direction at that point. Only the weak form of this equilibrium equation is employed in this theory. For this purpose, Eq. (120) is weighted and integrated over the cross-section:

$$\begin{aligned} \int \left(t \cdot \sigma_{x,x} + t \cdot \tau_{xs,s} + p_x \right) \cdot \Omega(s) \cdot ds = & \int \sigma_{x,x} \cdot \Omega(s) \cdot t \cdot ds \\ & + \int \tau_{xs,s} \cdot \Omega(s) \cdot t \cdot ds \\ & + \int p_x \cdot \Omega(s) \cdot ds \\ & = 0 \end{aligned} \tag{121}$$

where the weight function is the cross-sectional warping, represented by Ω. Each of the three terms in Eq. (121) is further developed in the following. The first term is modified by substitution of Eq. (119):

$$\int \sigma_{x,x} \cdot \Omega \cdot t \cdot ds = -E \cdot \frac{d^2F}{dx^2} \cdot \int \Omega^2 \cdot t \cdot ds = -EC_w \cdot \frac{d^2F}{dx^2} \tag{122}$$

The second term in Eq. (121) is rewritten by integration by parts:

$$\int \frac{d\tau_{xs}}{ds} \cdot t \cdot \Omega(s) \cdot ds = \left[\tau_{xs} \cdot t \cdot \Omega(s) \right] - \int \tau_{xs} \cdot \frac{d\Omega(s)}{ds} \cdot t \cdot ds \tag{123}$$

where the boundary term cancels. Eq. (123) is further rewritten by substitution of Eq. (112):

$$\int \tau_{xs} \cdot \frac{d\Omega(s)}{ds} \cdot t \cdot ds = \int \tau_{xs} \cdot (h - \bar{h}) \cdot t \cdot ds \tag{124}$$

This is expanded by substitution of Eq. (109):

$$\int \tau_{xs} \cdot (h - \bar{h}) \cdot t \cdot ds = G \cdot \phi' \cdot \int (h^2 - h\bar{h}) \cdot t \cdot ds - G \cdot F \cdot \int (h - \bar{h})^2 \cdot t \cdot ds \tag{125}$$

Introducing cross-section constants that are defined earlier, including the result from Eq. (114), yields:

$$\begin{aligned} & G \cdot \phi' \cdot \int (h^2 - h\bar{h}) \cdot t \cdot ds - G \cdot F \cdot \int (h - \bar{h})^2 \cdot t \cdot ds \\ & = G \cdot \phi' \cdot \left(J_h - J \right) - G \cdot F \cdot \left(J_h - 2 \cdot J + \int \bar{h}^2 \cdot t \cdot ds \right) \end{aligned} \tag{126}$$

This can be further simplified because Bredt's formula from St. Venant torsion yields

$$\int \bar{h}^2 \cdot t \cdot ds = \int \left(\frac{J}{2 \cdot t \cdot A_m} \right)^2 \cdot t \cdot ds = J^2 \cdot \frac{\int \frac{1}{t} ds}{4 \cdot A_m^2} = J \tag{127}$$

The third term in Eq. (121) defines the "warping load" on the cross-section:

$$m_\Omega = \int p_x \cdot \Omega(s) \cdot ds \tag{128}$$

In summary, Eq. (121) is written as the following differential equation:

$$-EC_w \cdot F'' - G \cdot \left(J_h - J \right) \cdot \phi' + G \cdot \left(J_h - J \right) \cdot F + m_\Omega = 0 \tag{129}$$

Combined Differential Equation

The differential equation for the shear-BVP in Eq. (117) and the differential equation for the axial-BVP in Eq. (129) are now combined. First Eq. (117) is solved for F':

$$F' = \left(\frac{J_h}{(J_h - J)} + \frac{J_{flanges}}{(J_h - J)} \right) \cdot \phi'' + \frac{m_x}{G \cdot (J_h - J)} \tag{130}$$

By differentiating twice, this equation is also employed to obtain an expression for F''':

$$F''' = \left(\frac{J_h}{(J_h - J)} + \frac{J_{flanges}}{(J_h - J)} \right) \cdot \phi'''' + \frac{m_x''}{G \cdot (J_h - J)} \tag{131}$$

The next step is to differentiate Eq. (129) once with respect to x and applying a minus-sign to it:

$$EC_w \cdot F''' + G \cdot \left(J_h - J \right) \cdot \phi'' - G \cdot \left(J_h - J \right) \cdot F' - m_\Omega' = 0 \tag{132}$$

Substitution of Eqs. (130) and (131) into Eq. (132) yields

$$EC_w \cdot \left(\left(\frac{J_h}{(J_h - J)} + \frac{J_{flanges}}{(J_h - J)} \right) \cdot \phi'''' + \frac{m_x''}{G \cdot (J_h - J)} \right)$$
$$+G \cdot (J_h - J) \cdot \phi'' - G \cdot (J_h - J) \cdot \left(\left(\frac{J_h}{(J_h - J)} + \frac{J_{flanges}}{(J_h - J)} \right) \cdot \phi'' + \frac{m_x}{G \cdot (J_h - J)} \right) \quad (133)$$
$$-m_\Omega' = 0$$

By re-arranging and defining the following auxiliary constants:

$$\alpha_o = \frac{J_h}{J_h - J} \quad (134)$$

$$\beta_o = \frac{J_{flanges}}{J_h} \quad (135)$$

$$\kappa_o = \frac{J_{flanges}}{J} \quad (136)$$

the following complete differential equation that contains both the axial-BVP and the shear-BVP (Hals 1993) is obtained:

$$EC_w \cdot \alpha_o (1 + \beta_o) \cdot \phi'''' - GJ \cdot (1 + \kappa_o) \cdot \phi'' = m_\Omega' + m_x - \frac{EC_w}{GJ_h} \cdot \alpha_o \cdot m_x'' \quad (137)$$

Problems without free flanges are characterized by $\beta_o = \kappa_o = 0$ and the homogeneous differential equation for such problems is:

$$EC_w \cdot \alpha_o \cdot \phi'''' - GJ \cdot \phi'' = 0 \quad (138)$$

which has the general solution:

$$\phi = C_1 + C_2 \cdot x + C_3 \cdot e^{k_o x} - C_4 \cdot e^{-k_o x} \quad (139)$$

where

$$k_o = \frac{GJ}{EC_w \alpha_o} \quad (140)$$

Once a solution to the differential equation is obtained, the unknown function $F(x)$ can be determined. Solving Eq. (129) yields

$$F = -\frac{m_\Omega}{G \cdot (J_h - J)} + \frac{EC_w \cdot F''}{G \cdot (J_h - J)} + \phi' \quad (141)$$

and substituting F'' from Eq. (130) differentiated once yields, when there are no free flanges:

$$F = -\frac{m_\Omega}{GJ_h} \cdot \alpha_o + \frac{EC_w \cdot \alpha_o^2}{GJ_h} \cdot \phi''' + \frac{EC_w \alpha_o}{GJ_h} \cdot \frac{m_x'}{GJ_h} \cdot \alpha_o + \phi' \quad (142)$$

This expression reveals the warping of the cross-section, but it is not needed to determine the bi-moment for axial stress computations. This is understood by first considering the definition of the bi-moment, which is:

$$B = -\int_A \sigma_x \cdot \Omega \, dA \tag{143}$$

Substitution of the expression for axial stress from Eq. (119) yields

$$B = \int_A E \cdot \frac{dF}{dx} \cdot \Omega^2 \, dA = EC_w \cdot F' \tag{144}$$

Instead of employing Eq. (142) to determine *F'*, it is possible to substitute F' from Eq. (130), which yields, when there are no free flanges:

$$B = EC_w \cdot \alpha_o \cdot \phi'' + \frac{EC_w}{GJ_h} \cdot \alpha_o \cdot m_x \tag{145}$$

The axial stress in the cross-section is obtained by combining Eq. (144) with Eq. (119):

$$\sigma_x = -\frac{B}{C_w} \cdot \Omega \tag{146}$$

The total torque is obtained by combining the expression for torque in Eq. (97) with the differential equation for shear in Eq. (117) and the differential equation for axial in Eq. (129). Substitution of *F* from Eq. (129) and then *F''* from the differentiated Eq. (117) into Eq. (116) yields:

$$T = -EC_w \cdot \alpha_o \cdot \phi''' + GJ \cdot \phi' - \frac{EC_w \cdot \alpha_o}{GJ_h} \cdot m_x' + m_\Omega \tag{147}$$

The shear stresses are obtained from Eq. (109):

$$\tau_{xs} = G \cdot \phi' \cdot h - G \cdot F \cdot (h - \overline{h}) \tag{148}$$

where the expression for *F* from Eq. (142) could conceivably be utilized. However, a better way of determining the stress stresses is to solve the statically indeterminate shear flow around the cell by enforcing compatibility.

References

Hals, T. E. (1993). *Tynnveggede staver*. Tapir.

Weberg, S. E. (1970). *Torsion og bøyning: massive, åpne og lukkede tverssnitt*. Institutt for statikk, NTH.